

# **Multi-stimuli responsive cyanostilbene derivatives: pH, amine vapor sensing and mechanoluminescence**

*Guangxi Huang<sup>†a</sup>, Xiaoyong Chang<sup>†c</sup>, Yuqing Jiang<sup>a</sup>, Bei Lin<sup>a</sup>, Bing Shi Li<sup>\*a</sup> and Ben Zhong Tang<sup>\*b</sup>*

*<sup>a</sup>Key Laboratory of New Lithium-Ion Battery and Mesoporous Material, Department of Chemistry and Environmental Engineering, Shenzhen University, 1066 Xueyuan Avenue, Nanshan, Shenzhen 518055, China. E-mail: [phbingsl@szu.edu.cn](mailto:phbingsl@szu.edu.cn); Fax: +86-755-26536141; Tel: +86-755-26558094*

*<sup>b</sup>Hong Kong Branch of Chinese National Engineering Research, Center for Tissue Restoration and Reconstruction, Department of Chemistry, The Hong Kong University of Science and Technology, Clear Water Bay, Kowloon, Hong Kong, China*

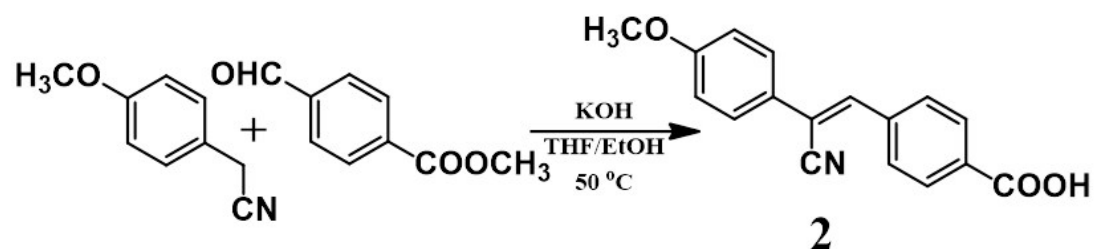
*<sup>c</sup>Department of Chemistry, Southern University of Science and Technology, 1088 Xueyuan Avenue, Nanshan, Shenzhen, 518055, China*

[†] G. X. Huang and X. Y. Chang contributed equally to this work.

### Instruments and methods

$^1\text{H}$  and  $^{13}\text{C}$  NMR spectra were recorded on a VNMRS 400 NMR spectrometer (Varian, USA). High resolution mass spectra (HR-MS) were recorded using an Autoflex III mass spectrometer (MALDI-TOF-MS, Bruker, Germany). Element analysis was performed using a vario EL cube elemental analyzer (Elementar, Germany). UV-Vis spectra were recorded using a UV-2600 spectrometer (Shimadzu, Japan). Absolute quantum efficiency was measured on an integrating sphere (C11347-11, Hamamatsu, Japan). Fluorescence lifetime was measured on a compact fluorescence lifetime spectrometer (C11367-11, Hamamatsu, Japan). IR spectra were recorded on a Spectrum Two FT-IR spectrophotometer (Perkin-Elmer, USA). The ML spectra were collected from a spectrometer of Acton SP2750 with a liquid-nitrogen-cooled CCD (SPEC-10, Princeton) as a power detector. The theoretical ground-state geometry and electronic structure of molecules **1-4** were optimized using the density functional theory (DFT) with B3LYP hybrid functional at the basis set level of 6-31+G(d). All the theoretical calculations were performed using Gaussian 03 package.<sup>1</sup>

Scheme S1. Synthetic route of compound **2**.



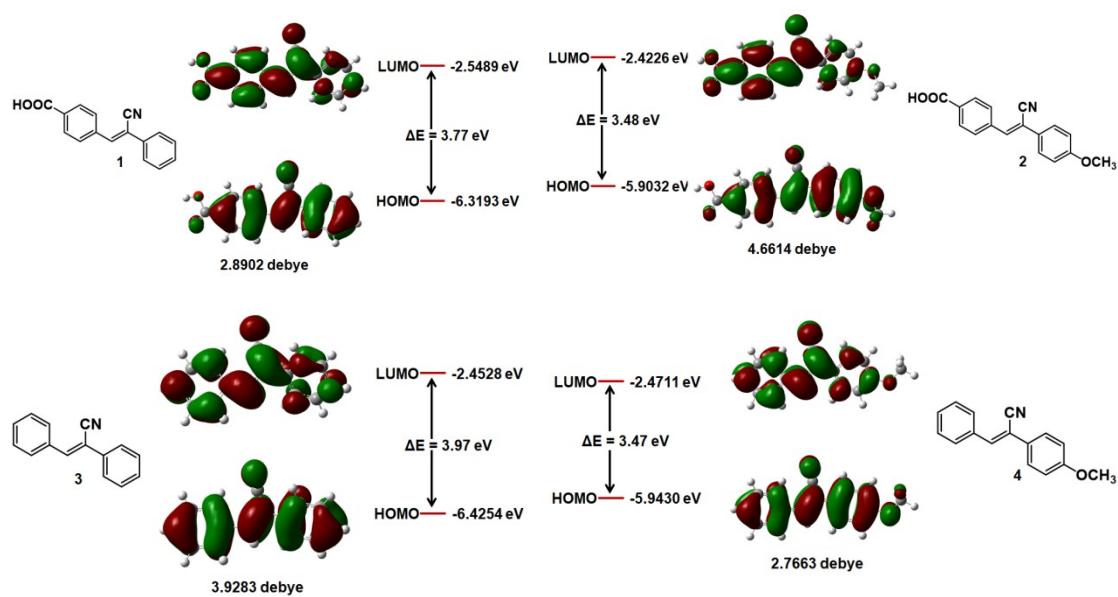


Figure S1. The HOMO and LUMO orbital distribution and dipole moment of **1-4** calculated by B3LYP/6-31+G(d).

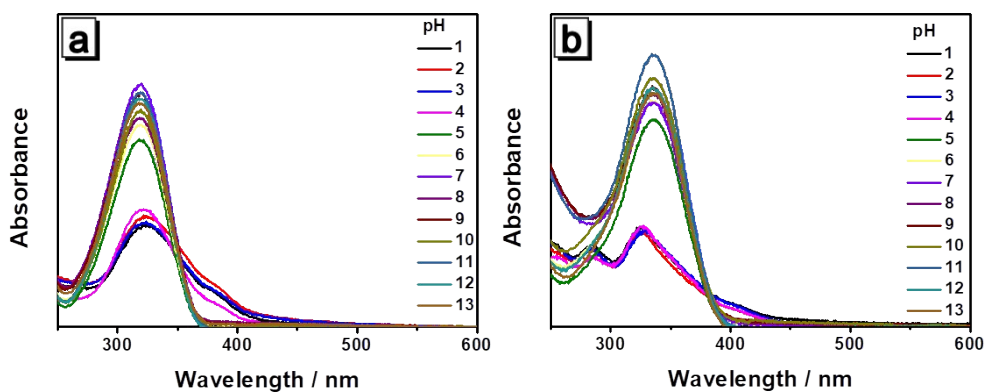


Figure S2. The absorption spectra of (a) **1** and (b) **2** in buffers with different pH values.

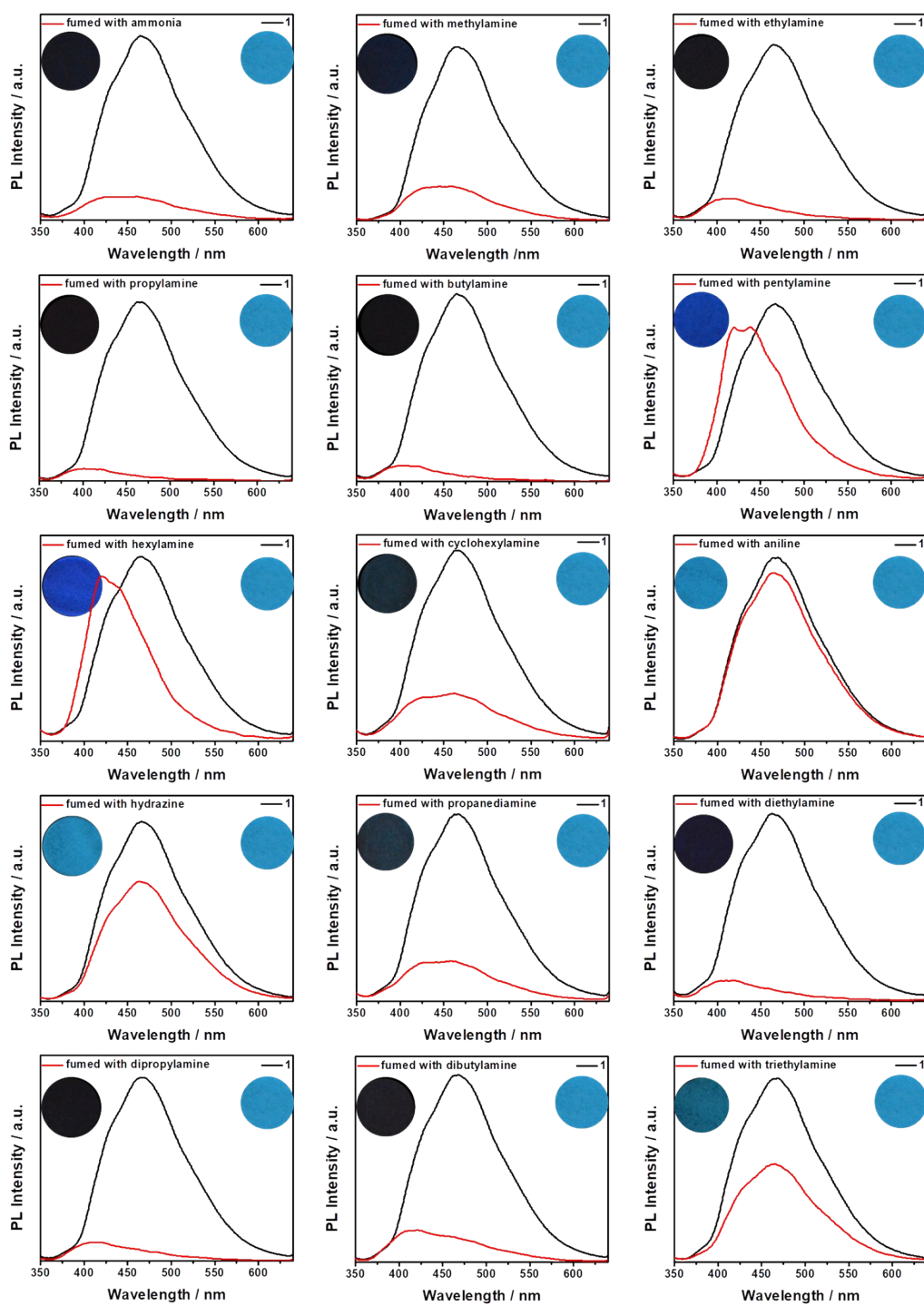


Figure S3. Fluorescent spectra of **1**-loaded test strips after dipped into different amine vapors for 5 s. Insets are the corresponding fluorescent photos.

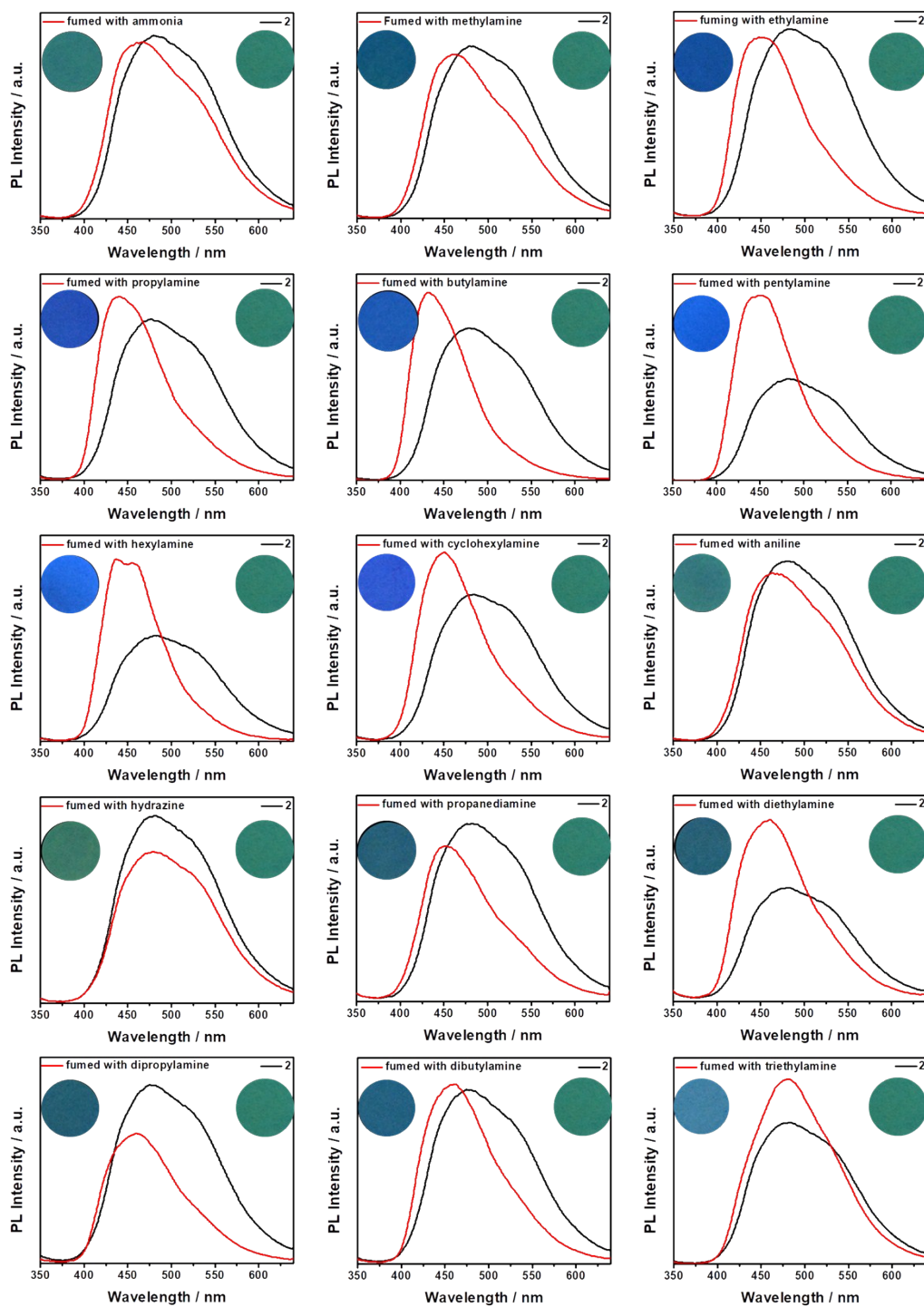


Figure S4. Fluorescent spectra of 2-loaded test strips after dipped into different amine vapors for 5 s. Insets are the corresponding fluorescent photos.

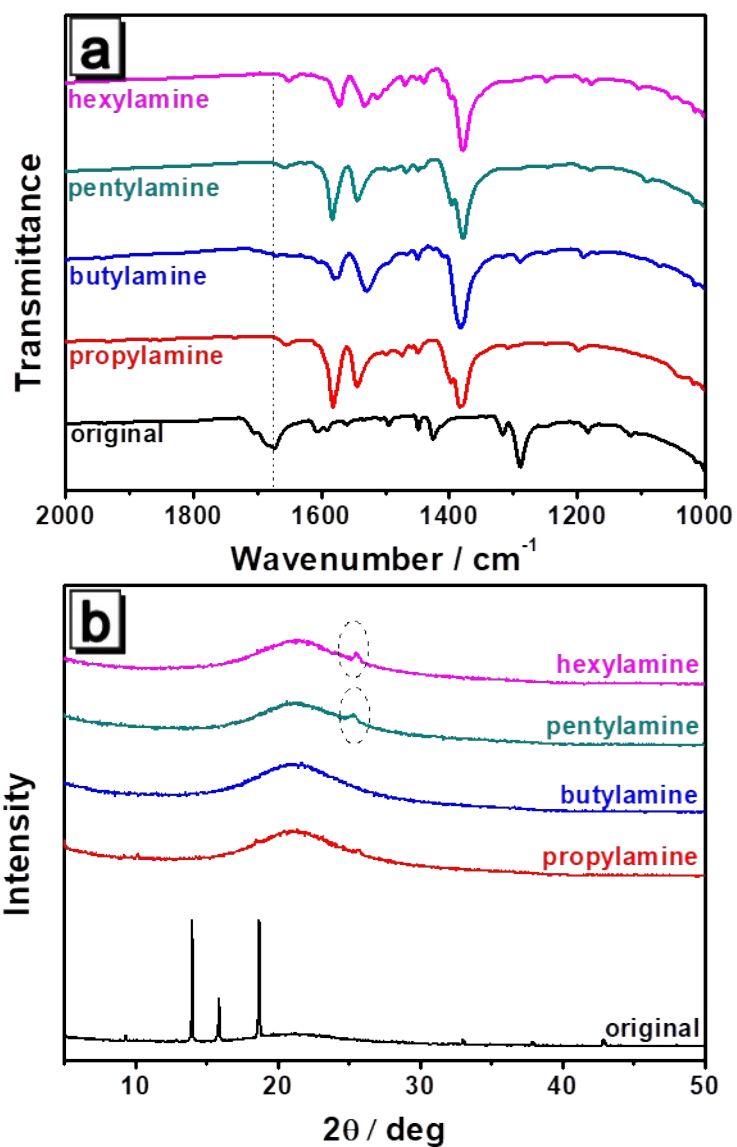


Figure S5. (a) IR spectra and (b) X-ray diffractograms of drop-casting films of **1** before and after fumed with different amine vapors. Films for IR spectra on  $\text{CaF}_2$  slides and X-ray diffractograms on quartz slides were prepared by 20  $\mu\text{L}$ , 20 mM and 100  $\mu\text{L}$ , 0.1 M THF solution of **1**, respectively.

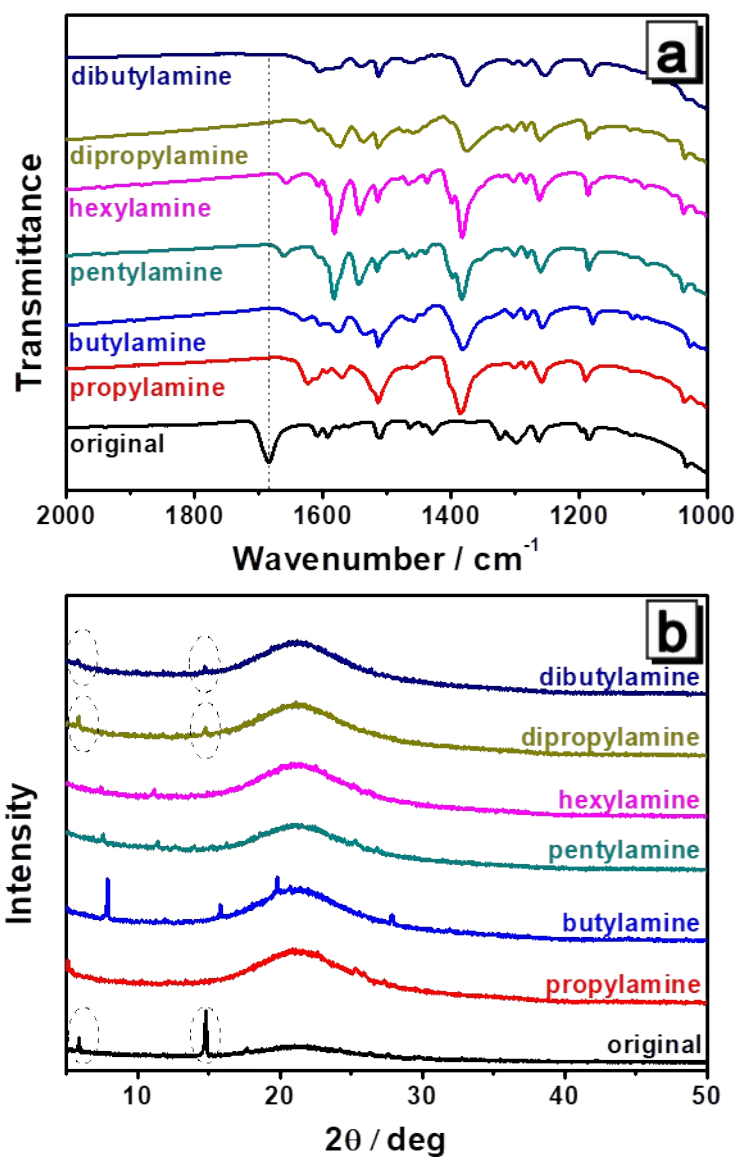


Figure S6. (a) IR spectra and (b) X-ray diffractograms of drop-casting films of **2** before and after fumed with different amine vapors. Films for IR spectra on  $\text{CaF}_2$  slides and X-ray diffractograms on quartz slides were prepared by 20  $\mu\text{L}$ , 20 mM and 100  $\mu\text{L}$ , 0.1 M THF solution of **2**, respectively.

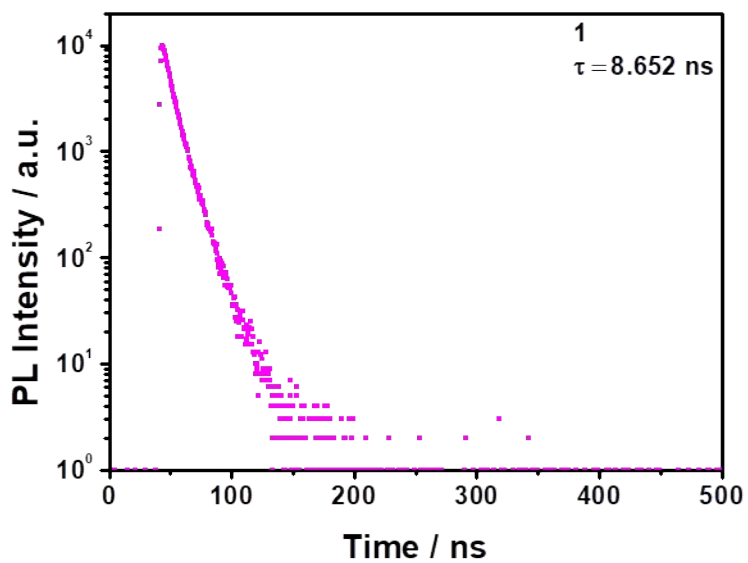


Figure S7. Fluorescence decay curve of single crystal 1.

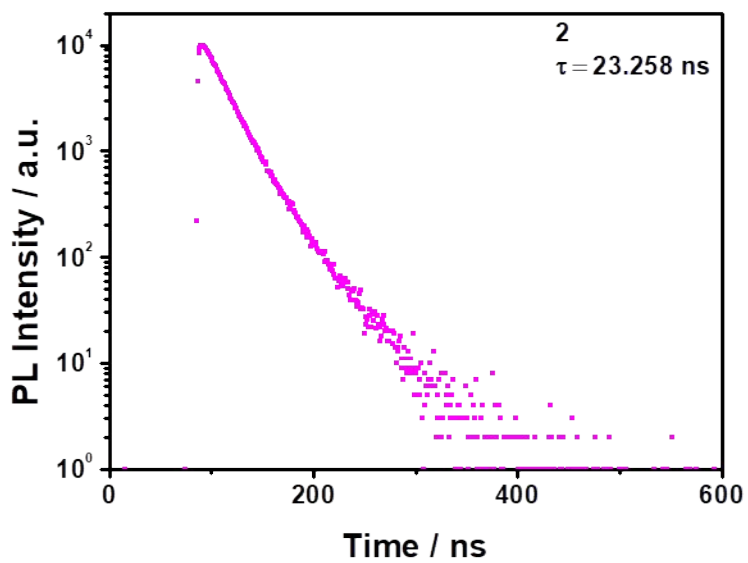


Figure S8. Fluorescence decay curve of single crystal 2.

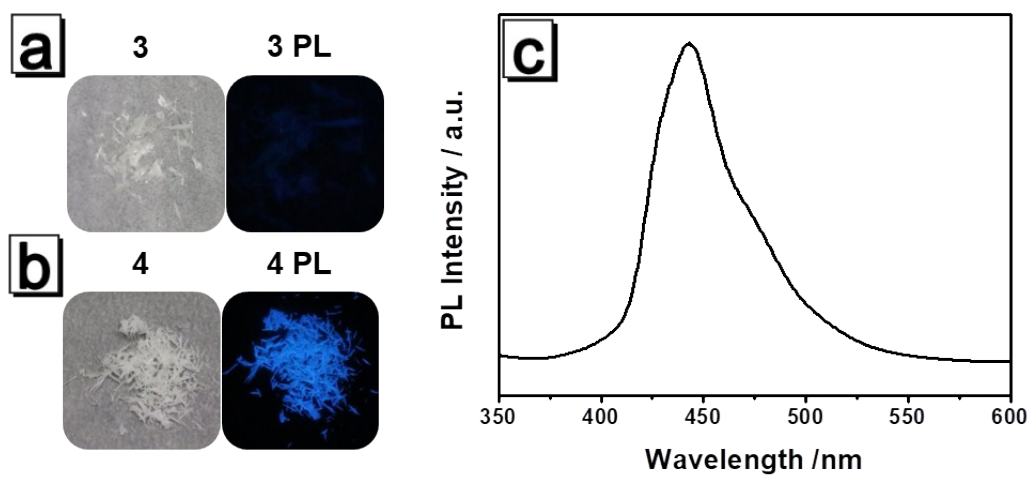


Figure S9. Photos of (a) **3** and (b) **4**, left: single crystal photo taken under natural light; right: single crystal photo taken under UV illumination. (c) Photoluminescence (PL) spectrum of crystal **4**.

Table S1. Single crystal data of **1-4**

	Compound <b>1</b>	Compound <b>2</b>	Compound <b>3</b>	Compound <b>4</b>
CCDC number	1887132	1887133	1949120	1949114
Formula	C16H11NO2	C17H13NO3	C15H11N	C16H13NO
Formula weight	248.26	279.28	205.25	235.27
	/g•mol <sup>-1</sup>			
Crystal system	Triclinic	Triclinic	Orthorhombic	Triclinic
Space group	P-1	P-1	Pbcn	P-1
T/K	173	294	268.39	170
Z	2	2	4	4
a/Å	3.8720(8)	6.8187(2)	23.0700(8)	7.24230(10)
b/Å	8.1785(15)	7.5408(2)	6.8458(2)	11.79970(10)
c/Å	19.377(4)	15.0920(3)	7.2886(2)	14.43200(10)
$\alpha$ /°	77.95(3)	82.274(2)	90	89.6560(10)
$\beta$ /°	87.16(3)	84.978(2)	90	82.1710(10)
$\gamma$ /°	88.41(3)	64.544(2)	90	89.4850(10)
V/Å <sup>3</sup>	599.3(2)	693.93(3)	1151.11(6)	1221.76(2)
$\rho$ /g•cm <sup>-3</sup>	1.381	1.337	1.184	1.279
$\mu$ /mm <sup>-1</sup>	0.092	0.756	0.531	0.630
F(000)	260.0	292.0	432	496
Reflections collected	9322	6032	3108	14790
Independent reflections	2715	2723	1135	4846
R <sub>int</sub>	0.0597	0.0207	0.0271	0.0218
R <sub>1</sub> (I > 2 $\sigma$ (I))	0.076	0.0415	0.0480	0.0369
wR <sub>2</sub>	0.1517	0.1233	0.1349	0.1053
GOOF	1.226	1.088	1.106	1.085

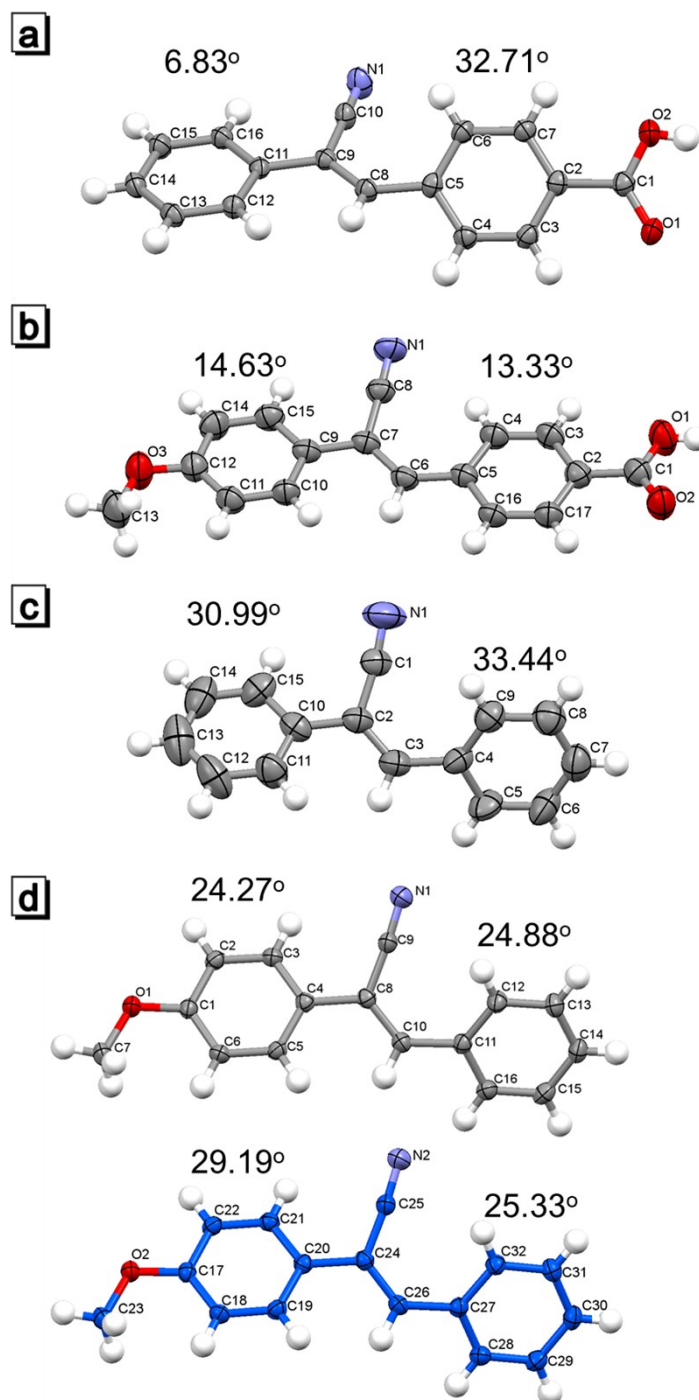


Figure S10. The molecular conformations with labels of carbon/oxygen/nitrogen atoms and dihedral angles between the phenyl ring and central ethene group of (a) **1**, (b) **2**, (c) **3** and (d) grey and blue conformation of **4**. Ellipsoids represent the 50% probability level. Hydrogen atoms are shown as spheres of arbitrary radii.

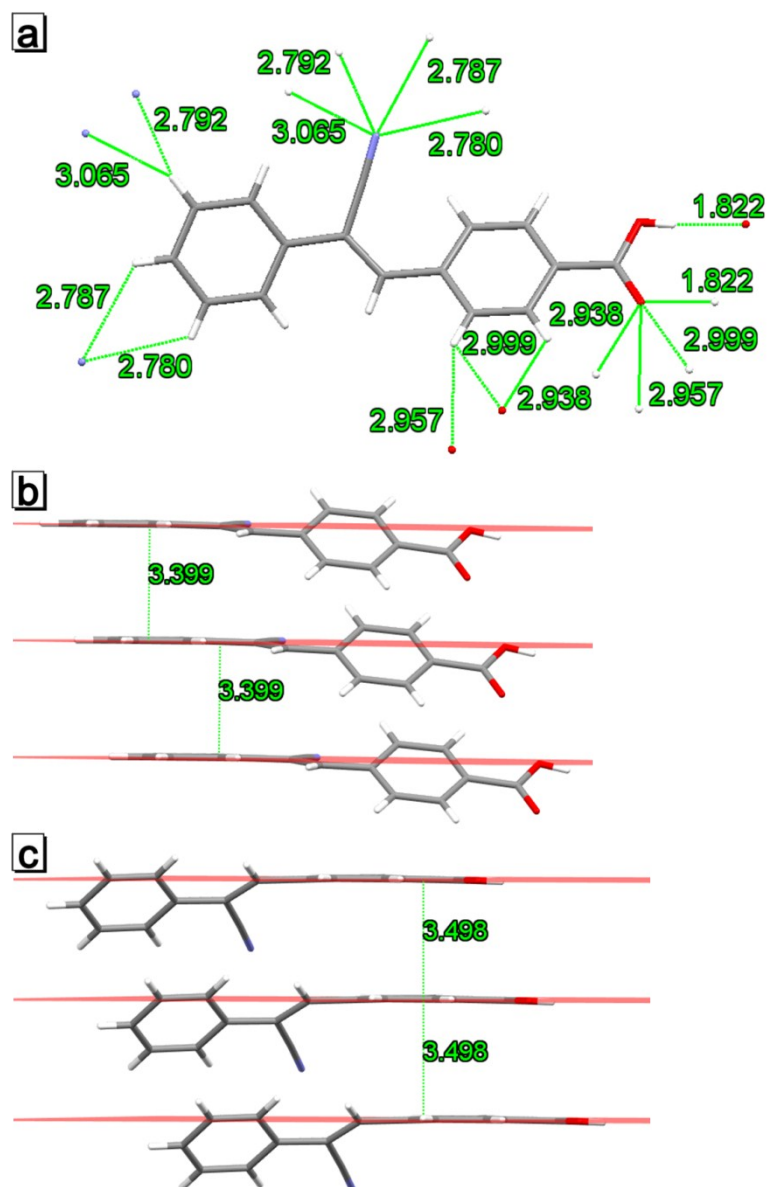


Figure S11. The detailed intermolecular interactions in crystal 1: (a) C-H...N, C-H...O and O-H...O interactions, (b) and (c)  $\pi$ - $\pi$  interactions. Distance of  $\pi$ - $\pi$  interaction is defined as distance between planes of benzene ring.

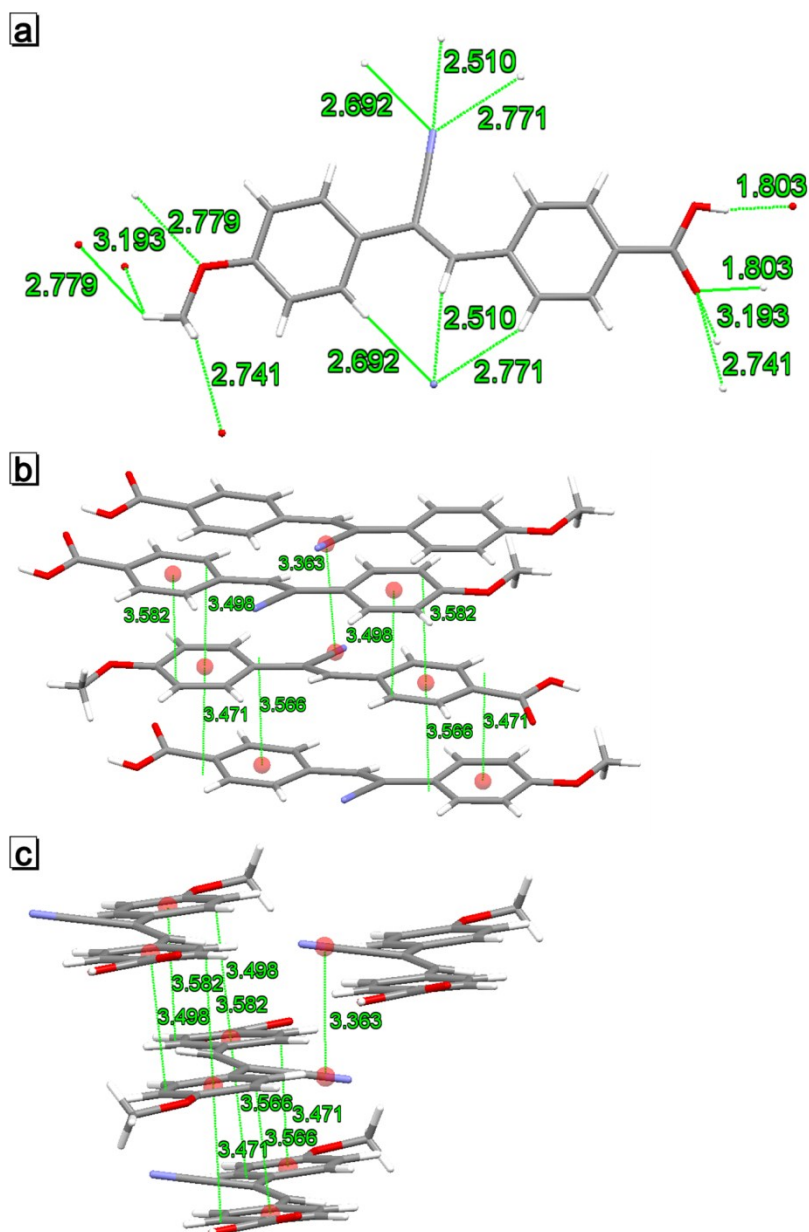


Figure S12. The detailed intermolecular interactions in crystal 2: (a) C-H...N, C-H...O and O-H...O interactions, (b)  $\pi$ - $\pi$  interactions and (c) side view of (b). Centroids of benzene rings are shown in red. Due to the existence of dihedral angle ( $3.48^\circ$ ) between adjacent aromatic rings, distance of  $\pi$ - $\pi$  interaction is defined as distance between centroid of one benzene ring and the plane of the other benzene ring. Thus, every  $\pi$ - $\pi$  interaction should have two distances.

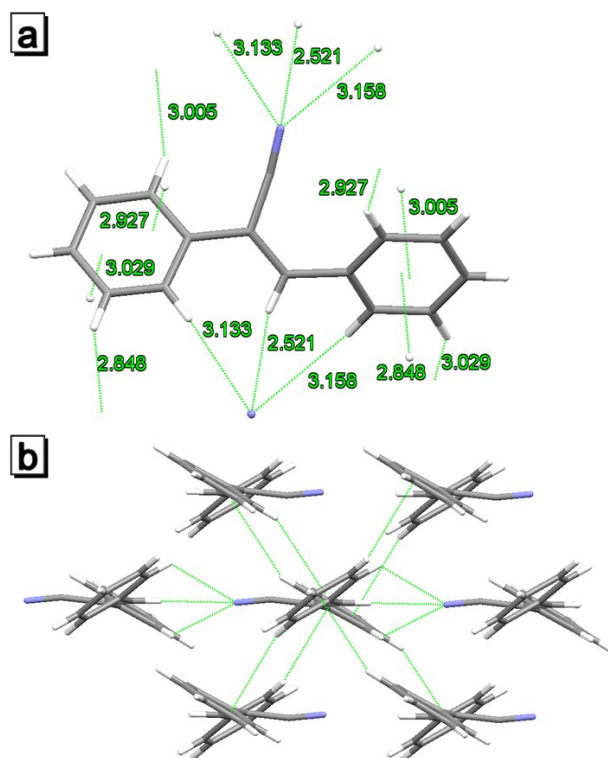


Figure S13. (a) The detailed intermolecular C-H...N and C-H... $\pi$  interactions in crystal **3**. Bond length of C-H... $\pi$  interaction is the distance between hydrogen atom and the plane of benzene ring. (b) Side view of Figure 5h, which revealed that molecule **3** had no  $\pi$ - $\pi$  interaction with upper or lower neighbouring molecule.



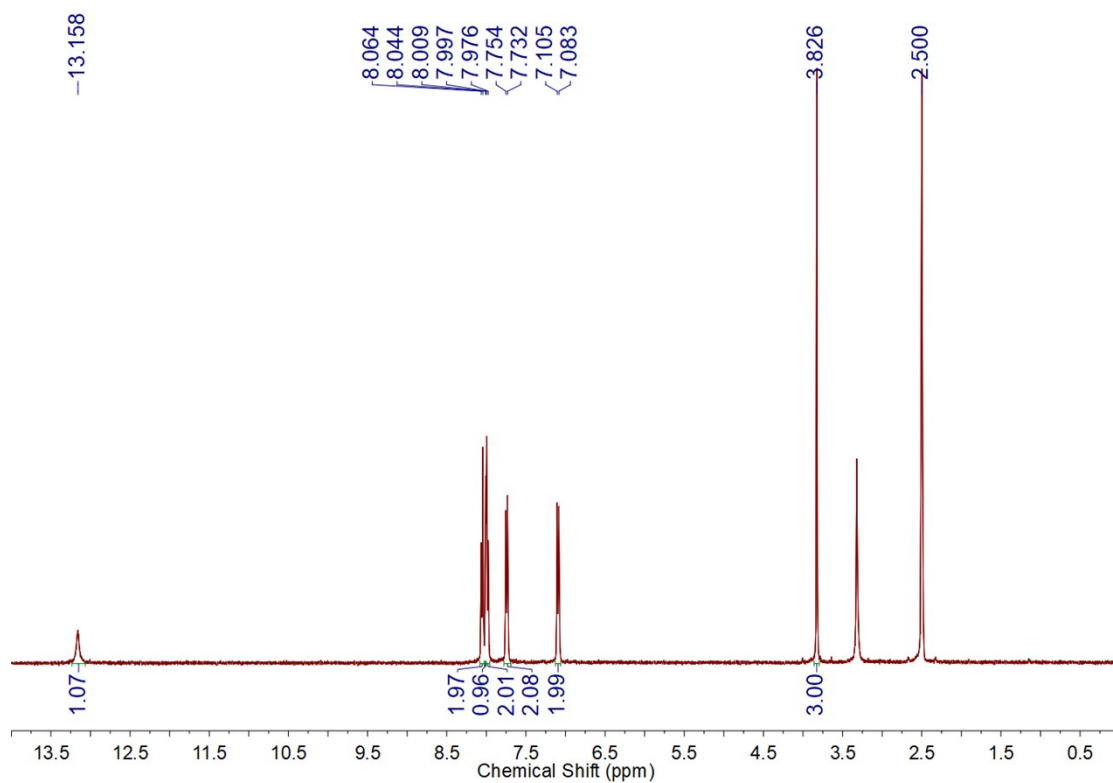


Figure S15.  $^1\text{H}$  NMR of compound **2**.

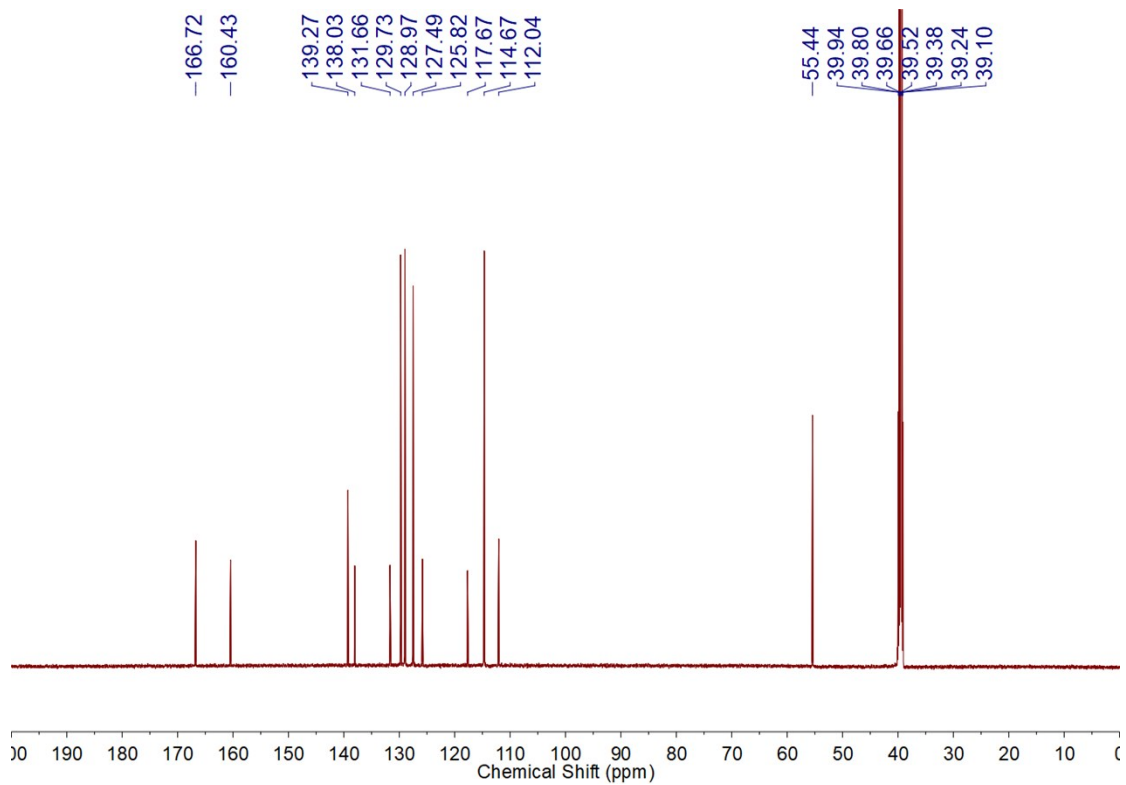


Figure S16.  $^{13}\text{C}$  NMR of compound **2**.

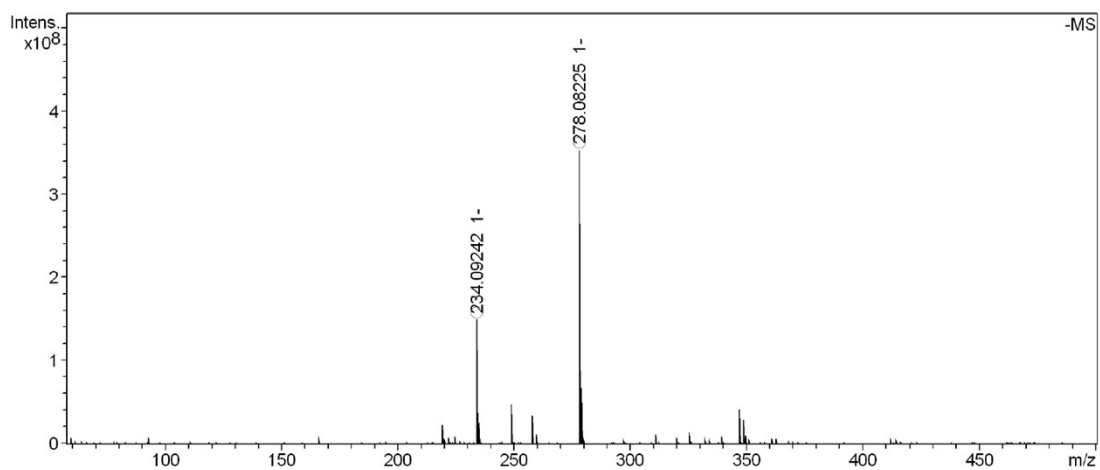


Figure S17. HRMS of compound **2**.

### References

1. Gaussian 03, Revision E.01, M. J. Frisch et al., Gaussian, Inc., Wallingford CT, 2009.